

# Antenna with Two Folded Strips Coupled to a T-Shaped Monopole

The-Nan Chang\* and Yi-Lin Chan

**Abstract**—An antenna designated mainly for cellular telephony purposes is presented. It covers one full band from 690 MHz to 2700 MHz with 6 dB return-loss criterion. The antenna is dimensioned 45 mm by 22.5 mm and is 0.8 mm in thickness. It is composed of a T-shaped monopole on the front-side and a meandered line on the back-side of an FR4 substrate. The T-shaped monopole is responsible for the high-band resonances. The meandered line is divided into three parts: the first part functions as a distributed inductor; the second part plays the role as a low-band resonator, and the third part is a tuning element. The distributed inductor and the low-band resonator are both folded strips in configuration, but with different spacing. The tuning element is used to improve the match so that one full band operation can be realized. To clarify the operational mechanism, modes separately generated from each part are analyzed and compared to modes of the proposed antenna.

## 1. INTRODUCTION

The development of the LTE 700/2300/2500 system has called for more bandwidth for the mobile antenna. The 900/1800 MHz dual-band operation was once popular three decades ago. Nowadays, the bandwidth often mixes the UHF-WLAN bands with the LTE bands [1–3]. Sometimes, the SHF-WLAN band may also be included [4–6]. For the configurations of the antennas, most of them involve the use of the meandered lines. In [5, 6], however, the log-periodic dipole arrays are adopted. As the lowest frequency is decreased to 690 MHz, it causes the main challenge to design the mobile antenna with an even limited space. Another discussed issue is to reduce the height of the antenna. In [7], the size of the antenna is 80 mm × 8 mm × 5.8 mm. In [8], the size of the antenna is 25 mm × 15 mm × 4 mm. In [9], the size of the antenna is 55 mm × 10 mm × 8 mm. All the three antennas are folded in structure to reduce the height of the antenna. Unfolded antennas with small size and low height are found in [10, 11]. In [10], the size of the antenna is 58 mm × 12 mm × 0.6 mm, while the antenna cannot cover the 850/900 GSM band. The size of the antenna in [11] is 35 mm × 10 mm × 0.8 mm, while the antenna requires a C-shaped ground plane. Instead of designing a very small antenna, a broadband antenna covering the full band from 690 MHz to 2700 MHz is proposed [12]. It allows the GPS band to be included in a mobile antenna. In [12], there is a chip inductor. In this study, the chip inductor is replaced by the distributed inductor which is implemented by a folded strip with a narrow spacing on the backside of a substrate. The first folded strip, or the inductor-strip, is directly connected to the system ground. Then, a second folded strip with a larger spacing than the inductor-strip is connected to the inductor-strip. The second folded strip is served as a resonator and is called the resonant-strip to distinguish it from the inductor-strip. The length of the second folded strip is tuned to operate as a quarter wavelength resonator which helps in lowering down the lowest operation frequency.

In brief, the antenna is featured to have a T-shaped driven monopole in the front-side and an inductor/resonator combination in the back-side of an FR4 substrate. The T-shaped strip-monopole

---

*Received 21 August 2017, Accepted 21 September 2017, Scheduled 5 October 2017*

\* Corresponding author: The-Nan Chang (tnchang@ttu.edu.tw).

The authors are with the Graduate Institute of Communication Engineering, Tatung University, Taiwan.

in [3, 4] is coupled to the coplanar meandered strips. The wide-band characteristics of a wide rectangular-monopole have been discussed in [12]. In this paper, the rectangular-monopole is modified to a T-shaped monopole and is coupled to the meandered strip on its backside. By this way, the length of the backside strip can be tuned to yield the lowest operation frequency to 690 MHz and the dual-band operation can easily be realized. The full-band antenna is obtained by adding a tuning stub close to the junction between the inductor-strip and the resonator-strip.

**2. ANALYSIS OF THE ANTENNA**

The size of the antenna shown in Fig. 1 is 22.5 mm in length and 45 mm in width. It is printed on both sides of an FR4 substrate, where the main ground plane covers an area of 97.5 mm by 45 mm. It is shown that there is a projected overlapped area. The layout patterns on the top side and on the bottom side are respectively shown in Fig. 2 and Fig. 3. In [13], two meandered strips are coupled on the same side of an FR4 substrate. The lowest frequency in [13] is 824 MHz. With the same sized antenna, we can design a full-band antenna lowest to 690 MHz. The antenna is simulated by the software of HFSS.

With the top-only antenna obtained by removing the backside strip from the proposed antenna,

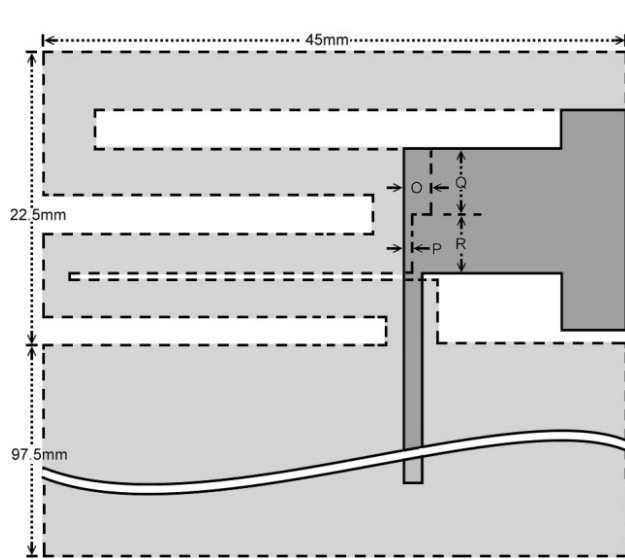


**Figure 1.** The proposed antenna is composed of a monopole (in dark-gray on the front side) and a meandered strip (in light-gray on the back side).

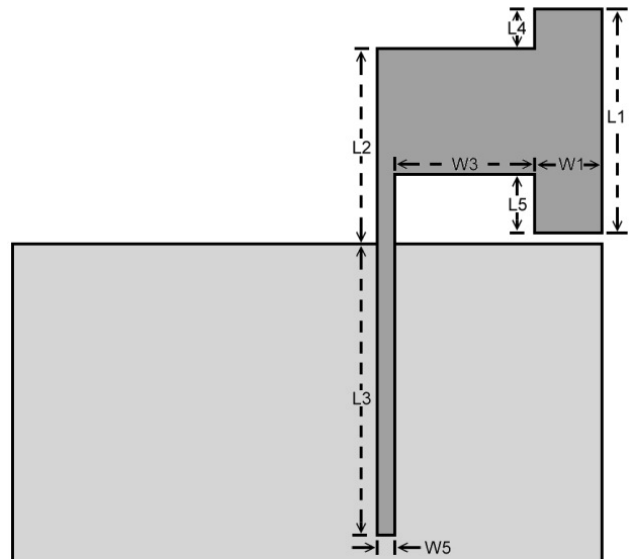


**Figure 2.** The driven monopole on the front-side of the substrate.

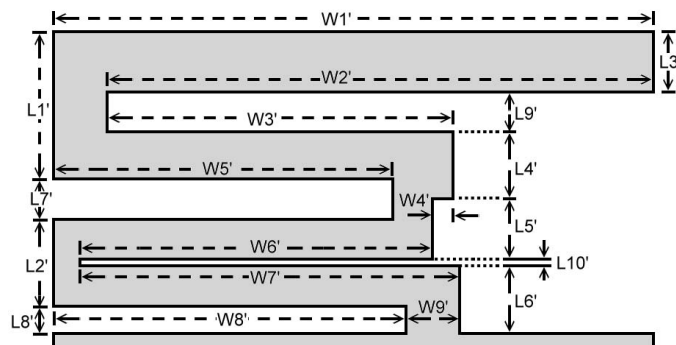


**Figure 3.** Two folded strips and one tuning strip on the backside of the substrate.

it is shown in Fig. 4 that the top-only antenna is poorly matched at the lower-part band. The top-only antenna generates the lowest operating frequency near 1100 MHz and it has a wider upper-part bandwidth above 1800 MHz. This characteristic is similar to the behavior of the rectangular monopole in [12]. By adding an L-like coupled backside strip (denoted by “Ref 1”) to the driven monopole, the center frequency on the lower-part band is lowered down from 1100 MHz to 803 MHz. The bandwidth in the lower-part band is from 770 MHz to 1050 MHz, and the bandwidth in the upper-part bandwidth is from 1685 MHz to 2570 MHz based on the 6-dB return loss criterion. The length of the “Ref 1” strip is 67.5 mm. To further decrease the lowest resonant frequency, we can increase the length of “Ref 1” to “Ref 2” and “Ref 3”. It is shown in Fig. 4 that the resonant frequency can be lowered to 690 MHz with the backside strip of “Ref 3”. However, the antenna with the backside strip of “Ref 3” suffers from poor match near 1400 MHz (less than 6 dB).

Up to now, two separated bands covering enough for the current mobile communication have been completed. Optionally, we can slightly modify the backside strip of “Ref 3” so that the GPS band can also be included. It is noted from Fig. 3 that a tuning stub with  $L4'$  in length and  $W4'$  in width is

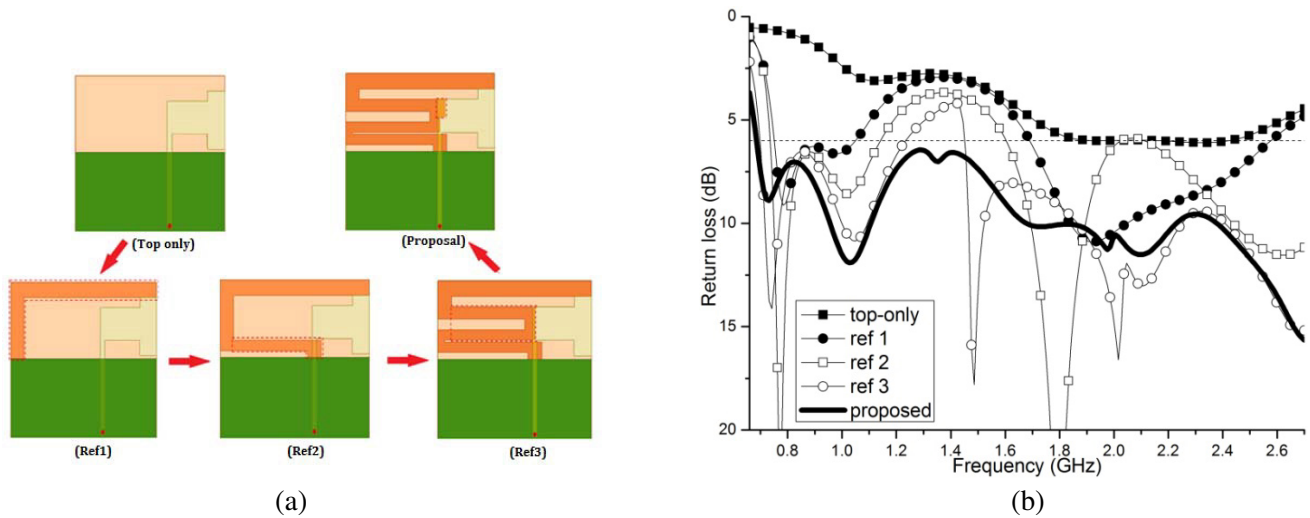


**Figure 4.** Antenna performances with the same driven monopole and different backside strips, (a) various backside-strip patterns, (b) the return-loss responses.

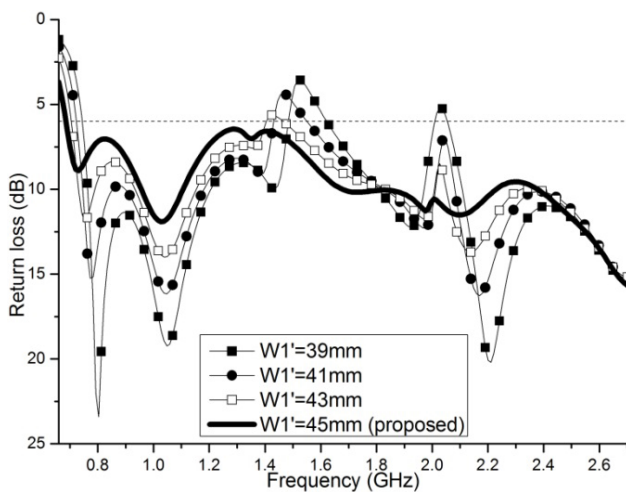


**Figure 5.** Return-loss responses of the proposed antenna by varying the length of  $W1'$ .

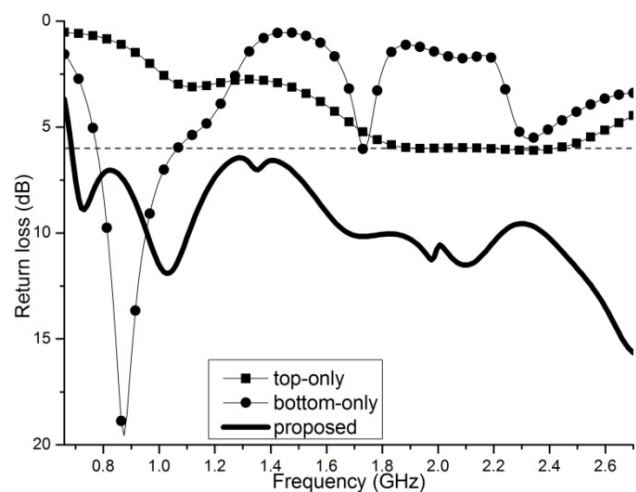


**Figure 6.** Return-loss of the proposed, the top-only, and the bottom-only antenna.

included in the backside strip. It is also shown in Fig. 4 that the stub can effectively improve the match near 1400 MHz. The normalized input impedance of the antenna at 1400 MHz is  $0.37 + j0.7\Omega$  before adding the stub and it becomes  $0.4 - j0.37\Omega$  after tagging the stub to the meandered line. Therefore, the stub is equivalent to a series capacitance seen from the input line. In [12], we used two wide tuning stubs and the two stubs were modelled as the shunt capacitance for a wide range. In this paper, it is studied that the tuning stub only works for a narrow frequency range near 1400 MHz. The antenna with VSWR less than 3 within the whole 690–2700 MHz bandwidth is, therefore, featured to have a T-shaped monopole on the front-side and a backside-strip of “Ref 4” on the rear side of the substrate. In the proposed antenna,  $W1' = 45$  mm is associated with “Ref 4”. The return-loss response of the proposed antenna by varying the length of  $W1'$  is shown in Fig. 5. It is shown in Fig. 5 that the three optimized resonant frequencies at 730 MHz, 1370 MHz, and 2100 MHz are all shifted higher as  $W1'$  is decreased. On the other hand, the resonant frequencies at 1030 MHz, 1990 MHz, and 2700 MHz are insensitive to the variation of  $W1'$ .

In the proposed antenna, there are three types of strip on the backside of the substrate. They are the tuning strip, inductor-strip and resonant-strip. It has been demonstrated that the tuning strip is responsible for the match between the upper-part and lower-part bands. The six resonant frequencies of the proposed antenna, therefore, are coupled from the modes of the top-strip, inductor-strip, and resonant-strip. In the proposed antenna, the adjacent spacing is  $L9' = 3$  mm and  $L10' = 0.5$  mm, respectively in the resonant folded strip and inductor folded strip. The smaller spacing makes the inductor-strip not be used to generate any resonant modes. It can also be confirmed later by studying the current distribution on the backside strip. In the proposed antenna, the backside strip is parasitically coupled to the top-only antenna. However, one can also analyze a driven bottom-only antenna. The driven bottom-only antenna is featured to have only the backside strip and is excited by a source at the ground edge.

In Fig. 6, the return-loss responses of the top-only antenna, the bottom-only antenna, and the proposed antenna are compared to each other. They are all simulated with  $W1' = 45$  mm. It is shown that there is one clear resonant frequency at 1100 MHz in the top-only antenna, and there are three resonant frequencies at 870 MHz, 1740 MHz, and 2350 MHz in the bottom-only antenna. The top-only antenna also exhibits a broadband characteristic from 1750 MHz to 2550 MHz. The proposed antenna contains the modes coupled from the top-only and bottom-only antennas. Among them, the three frequencies at 730 MHz, 1370 MHz, and 2100 MHz are shifted respectively from the corresponding modes on the backside-strip. The reason can better be understood by also referring to Fig. 5 as the three frequencies are shifted up when  $W1'$  is decreased. We may also reasonably judge that the mode at 1100 MHz in the top-only antenna could possibly be shifted to 1030 MHz in the proposed antenna. In Fig. 5, the change of the length of the backside-side has little effect on mode at 1030 MHz as it is

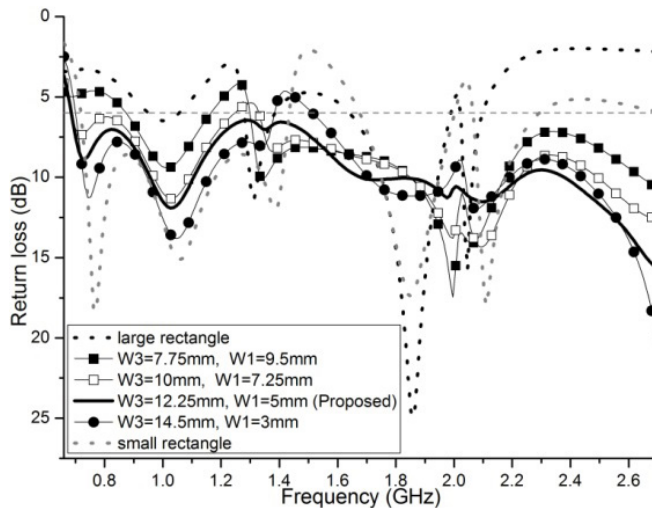


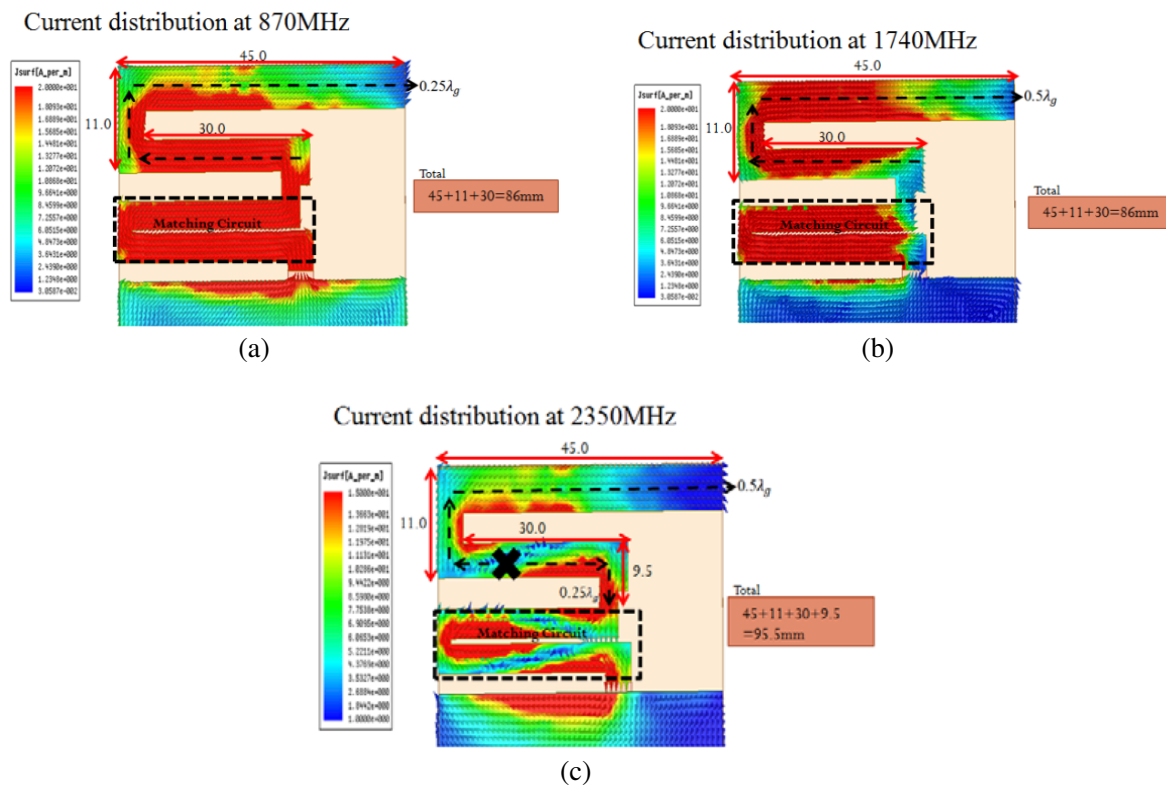
**Figure 7.** Return loss of the antenna by varying  $W1$  and  $W3$ .

originated from the top-strip. On the other hand, the change of the length of the backside-side has more effect on modes at 730 MHz, 1370 MHz, and 2100 MHz as they are originated from the backside-strip.

In Fig. 7, the return-loss of the proposed antenna is investigated by varying the parameters related to the top-side only. Two special cases are also included. The “large rectangle” is with width of  $(W3 + W1)$  and length of  $(L1)$ . The “small rectangle” has the same width as the large rectangle, but with a length of  $(L1 - L4 - L5)$ . It is shown that both rectangles cannot meet the 6-dB return-loss criterion over the upper-part band. The use of the T-shaped monopole can effectively improve the match over the upper-part band.

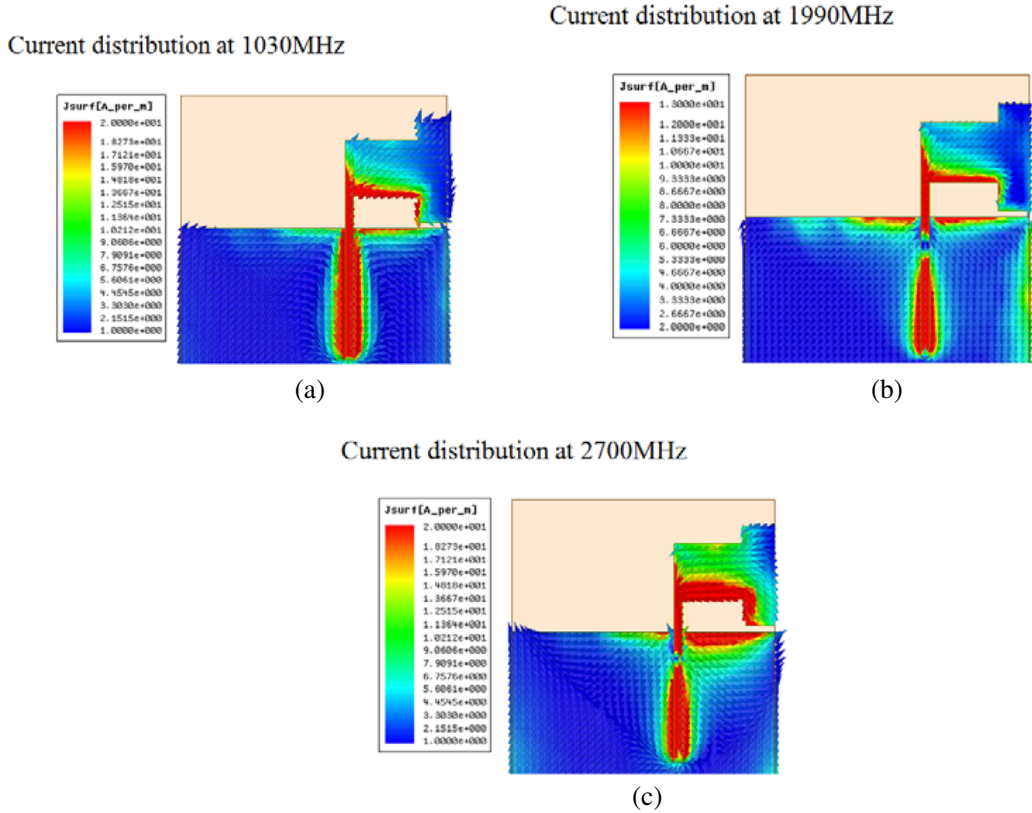
Since the ratio of the three resonant frequencies from the bottom-only antenna is near 1 : 2 : 3, it is reasonable to conclude that the antenna is operated as  $0.25\lambda_g$ ,  $0.5\lambda_g$ , and  $0.75\lambda_g$  radiators, respectively at the three frequencies. The current distributions at three resonant frequencies of the bottom-only antenna are shown in Fig. 8. Currents in the marked regions function as the match circuit. For the resonant path at 870 MHz, it is shown that the current flows in the arrow’s direction and reaches a null (minimum current) at the end, which is the quarter-wavelength distribution. For the resonant path at 1740 MHz, there are two nulls, and the current flows in the same direction resulting in a half-wavelength distributed pattern. For the resonant path at 2350 MHz, a cross sign,  $x$ , is highlighted. The current reverses its direction at this point making the current distributed as the  $0.75\lambda_g$  radiator. One half has a length of  $0.5\lambda_g$ , and the other half has a length of  $0.25\lambda_g$ .

The current distributions at three frequencies of the top-only antenna are shown in Fig. 9. The current distributes only part of the T-shaped region at 1030 MHz and 1990 MHz, and distributes most of the T-shaped region at 2700 MHz. The current distributions at six resonant frequencies of the proposed antenna are shown in Fig. 10. It is expected that most of the current is concentrated on the backside at 730 MHz and is concentrated on the topside at 2700 MHz. In between 730 MHz and 2650 MHz, the current is distributed on both sides due to mutual coupling.

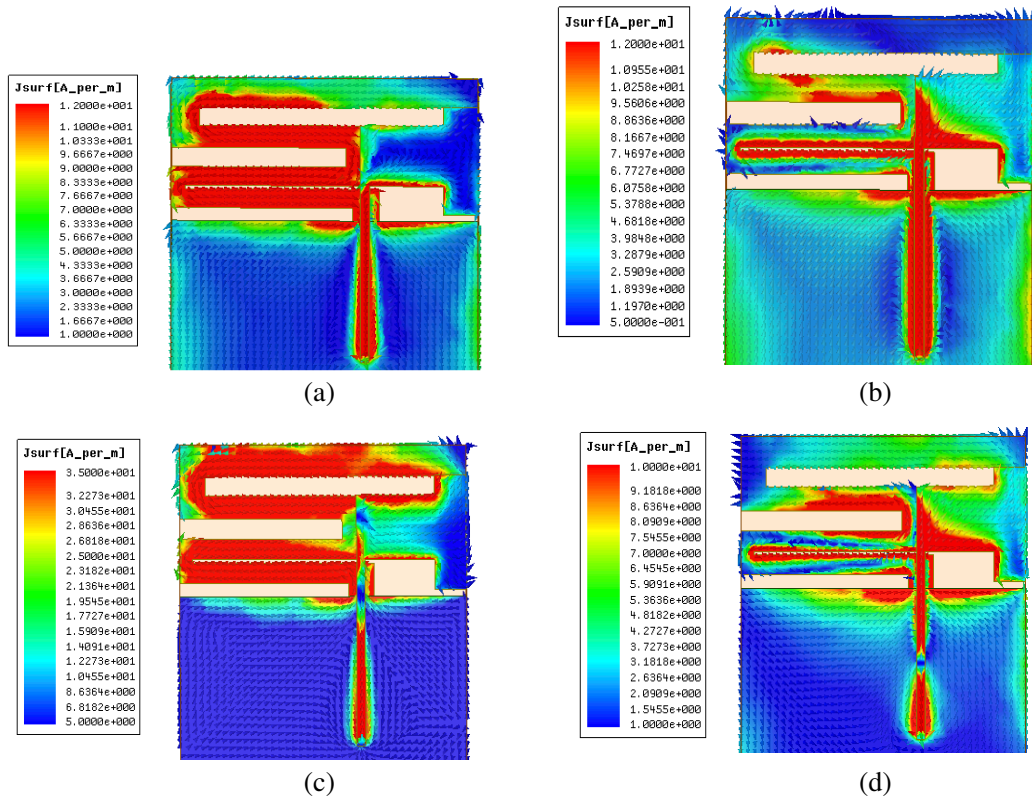


**Figure 8.** Current distribution of the bottom-only antenna at (a) 870 MHz, (b) 1740 MHz, and (c) 2350 MHz.





**Figure 9.** Current distribution of the top-only antenna at (a) 1030 MHz, (b) 1990 MHz, and (c) 2700 MHz.



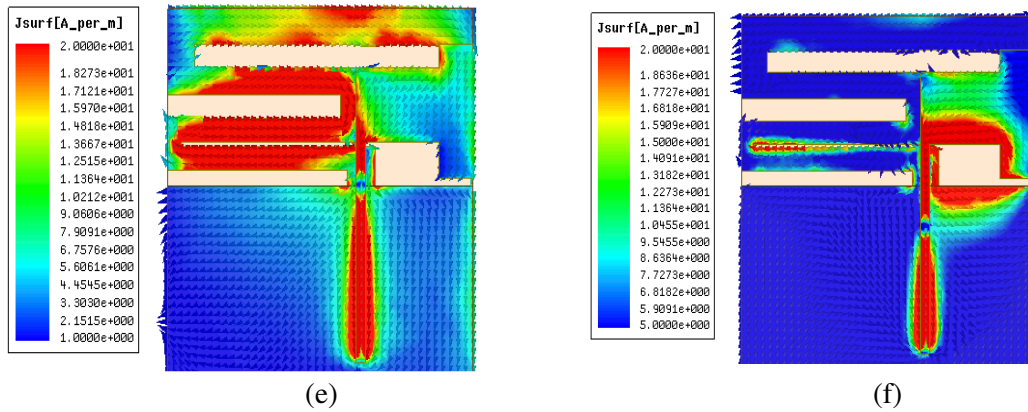


**Figure 10.** The current distribution of the proposed antenna at (a) 730 MHz, (b) 1030 MHz, (c) 1370 MHz, (d) 1990 MHz, (e) 2100 MHz, and (f) 2700 MHz.

### 3. MEASUREMENT

The main parameters of the proposed antenna are listed in Tables 1, 2, and 3. Table 1 and Table 2 respectively display the parameters on the topside and backside of the substrate. For clearance, the

**Table 1.** Parameters on the topside of the substrate.

Parameters	Values	Parameters	Values
$W1$	5 mm	$L2$	15 mm
$W3$	12.25 mm	$L3$	22.3 mm
$W5$	1.35 mm	$L4$	3 mm
$L1$	17 mm	$L5$	4.5 mm

**Table 2.** Parameters on the backside of the substrate.

Parameters	Values	Parameters	Values
$W1'$	45 mm	$L1'$	11 mm
$W2'$	41 mm	$L2'$	6.5 mm
$W3'$	26 mm	$L3'$	4.5 mm
$W4'$	1.5 mm	$L4'$	5 mm
$W5'$	25.5 mm	$L5'$	4.5 mm
$W6'$	26.5 mm	$L6'$	5 mm
$W7'$	28.5 mm	$L7'$	3 mm
$W8'$	26.5 mm	$L8'$	2 mm
$W9'$	4 mm	$L9'$	3 mm
		$L10'$	0.5 mm

**Table 3.** Parameters on the overlapped area.

Parameters	Values	Parameters	Values
$O = L4'$	5 mm	$P$	0.75 mm
$Q$	2.25 mm	$R = L5'$	4.5 mm

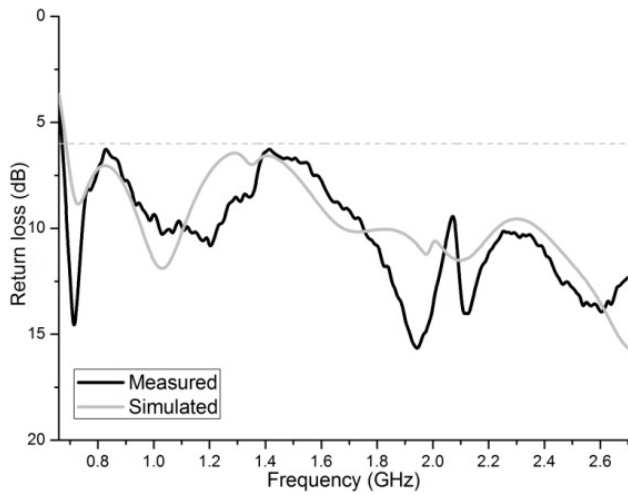


**Figure 11.** Simulated and measured return loss of the proposed antenna.

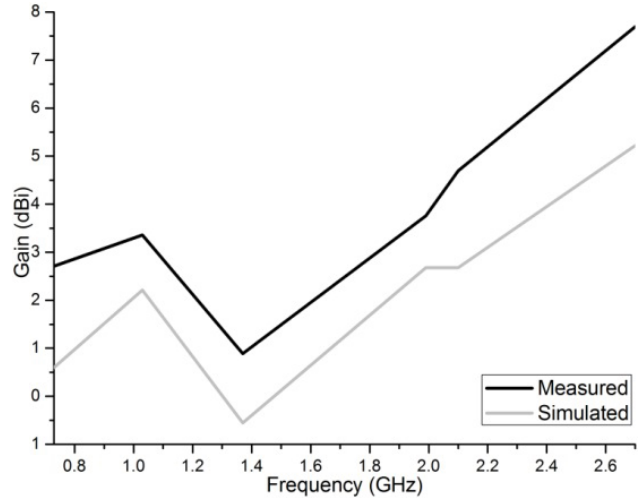


**Figure 12.** Simulated and measured gains of the proposed antenna.

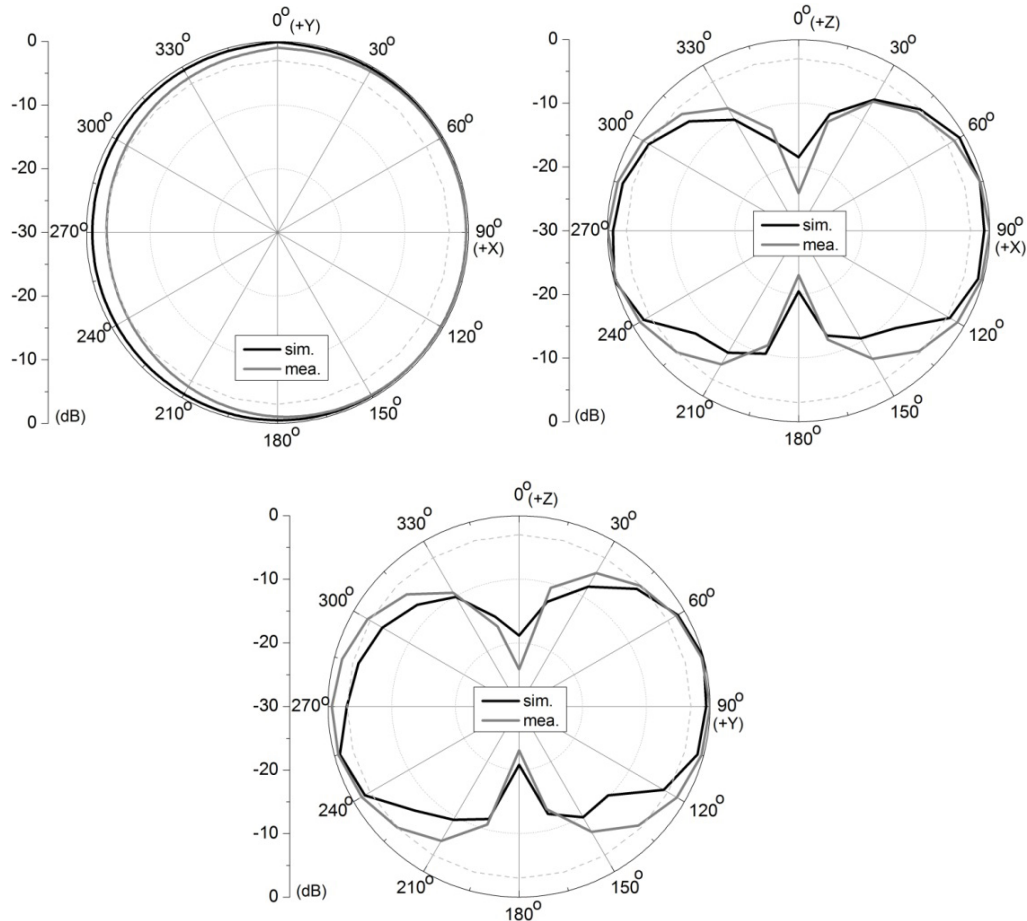
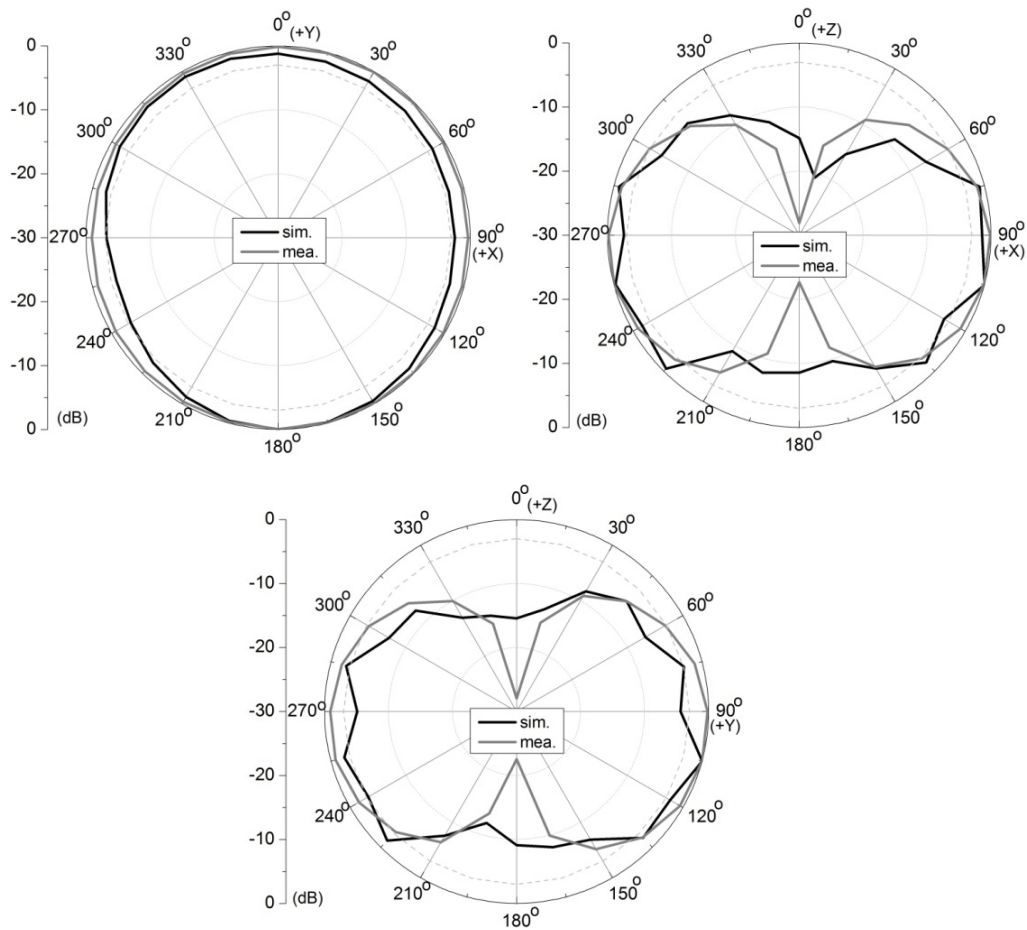


**Figure 13.** Simulated and measured patterns of the proposed antenna at 730 MHz.

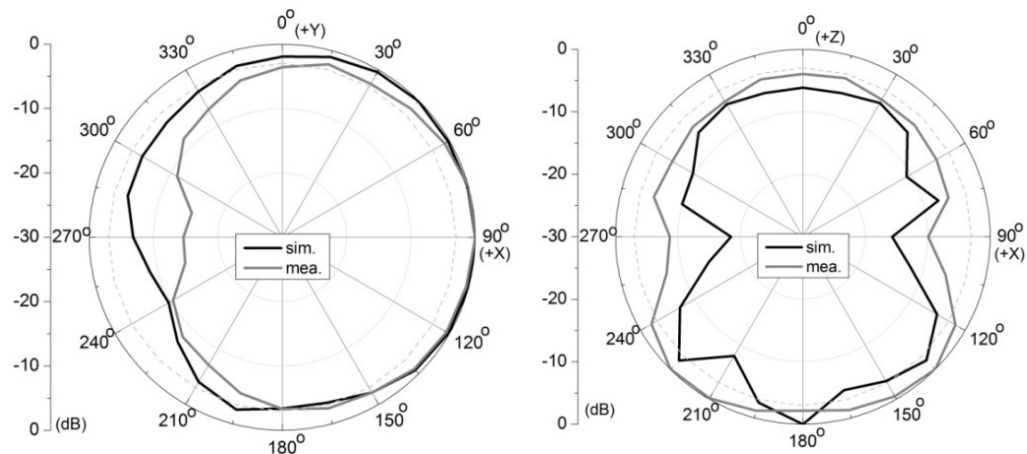
parameters related to the projected overlapped area of both sides are listed in Table 3. Fig. 11 shows a comparison of the simulated and measured return losses of the antenna. From 660 MHz to 2700 MHz, the measured return loss values are above 6 dB. The simulated and measured gains are respectively



shown in Fig. 12. It is shown that the trends of the simulated and measured gain responses agree well. Meanwhile, the return-loss response in Fig. 11 and the gain response in Fig. 12 are also compatible with each other. In Fig. 11, the antenna is relatively better-matched at 1000 MHz and poorly-matched at 1400 MHz. Beyond 1400 MHz, the antenna is generally getting more and more matched as the frequency is increased. In Fig. 12, it is shown that the antenna has a local maximum gain at the better-matched frequency of 1000 MHz and a local minimum gain at the poorly-matched frequency of 1400 MHz. Beyond



**Figure 14.** Simulated and measured patterns of the proposed antenna at 1370 MHz.



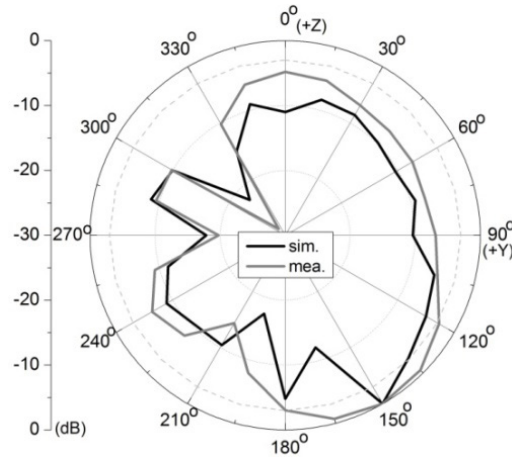


**Figure 15.** Simulated and measured patterns of the proposed antenna at 2690 MHz.

1400 MHz, the gain goes upwards. The measured and simulated patterns of the antenna at 730 MHz, 1370 MHz and 2650 MHz are, respectively, shown in Figs. 13, 14, and 15. In simulated pattern, the antenna is situated in  $yz$ -plane with  $x$ -axis points in the boresight direction. The antenna exhibits an omnidirectional pattern at 730 MHz and 1370 MHz. At 2690, the measured pattern can still be predicted by the simulation. At low frequency, the radiation is contributed from the meandered line part of the antenna. It simply behaves as a quarter-wavelength resonant monopole. Therefore, it generates an ideal pattern. The pattern usually deteriorates with frequency as modes from both the meandered line (the higher-order resonance) and the monopole contribute to the radiation.

#### 4. CONCLUSION

The paper is a continuous research following the work in [12]. We have successfully completed the full-band antenna without using the chip inductor. The chip-inductor is replaced by a distributed inductor-strip. Following the distributed inductor-strip, the resonant-strip is connected together. Both strips are constructed as folded strip in configuration. The resonant-strip, being a meandered line, is easy to generate one fundamental and two harmonic modes. The inductor-strip, however, does not generate any resonant frequencies. The use of two-folded strips with different spacing introduced in this paper is new to promise that each strip realizes its respective function.

The T-shaped monopole inherently exhibits a wideband characteristic from 1750 to 2550 MHz in addition to a fundamental resonant mode at 1100 MHz. The monopole-type antenna is suitable to provide higher-part bandwidth. To promise a wideband from 690 to 2700 MHz, a tuning stub is also added to the backside strip. The use of monopole broadside-coupled to the meandered line has been introduced in [12]. The two broadside-coupled different-typed resonators are rarely seen in the literature. In [13], the edge coupling between two meandered lines is used. The antenna in [13] is of the same size as ours, but it cannot cover the lowest resonant frequency to 690 MHz. The proposed antenna is simple in configuration and is ready for LTE/WWAN/GPS application.

#### ACKNOWLEDGMENT

We appreciate Dr. J. M. Lin redrawing some of the figures.

#### REFERENCES

1. Chu, F.-H. and K.-L. Wong, "Planar printed strip monopole with a closely-coupled parasitic shorted strip for eight-band LTE/GSM/UMTS mobile phone," *IEEE Transactions on Antennas and Propagation*, Vol. 58, No. 10, 3426–3429, 2010.

2. Chen, Y.-S. and T.-Y. Ku, "Development of a compact LTE dual-band antenna using fractional factorial design," *IEEE Antennas and Wireless Propagation Letters*, Vol. 14, 1097–1100, 2015.
3. Ban, Y.-L., C.-L. Liu, J. L.-W. Li, J. Guo, and Y. Kang, "Small-size coupled-fed antenna with two printed distributed inductors for seven-band WWAN/LTE mobile handset," *IEEE Transactions on Antennas and Propagation*, Vol. 61, No. 11, 5780–5784, 2013.
4. Liu, H. J., R. L. Li, Y. Pan, X. L. Quan, L. Yang, and L. Zheng, "A multi-broadband planar antenna for GSM/UMTS/LTE and WLAN/WiMAX handsets," *IEEE Transactions on Antennas and Propagation*, Vol. 62, No. 5, 2856–2860, 2014.
5. Casula, G. A., P. Maxia, G. Montisci, G. Mazzarella, and F. Gaudiomonte, "A printed LPDA fed by a coplanar waveguide for broadband applications," *IEEE Antennas and Wireless Propagation Letters*, Vol. 12, 1232–1235, 2013.
6. Casula, G. A., G. Montisci, P. Maxia, G. Valente, A. Fanti, and G. Mazzarella, "A low-cost dual-band CPW-fed printed LPDA for wireless communications," *IEEE Antennas and Wireless Propagation Letters*, Vol. 15, 1333–1336, 2016.
7. Wang, Y. and Z. Du, "Wideband monopole antenna with less nonground portion for octa-band WWAN/LTE mobile phones," *IEEE Transactions on Antennas and Propagation*, Vol. 64, No. 1, 383–388, 2016.
8. Ban, Y.-L., C.-L. Liu, Z. Chen, J. L.-W. Li, and K. Kang, "Small-size multiresonant octaband antenna for LTE/WWAN smartphone applications," *IEEE Antennas and Wireless Propagation Letters*, Vol. 13, 619–621, 2014.
9. Chu, F.-H. and K.-L. Wong, "Internal coupled-fed dual-loop antenna integrated with a USB connector for WWAN/LTE mobile handset," *IEEE Transactions on Antennas and Propagation*, Vol. 59, No. 11, 4215–4221, 2011.
10. Hsu, C.-K. and S.-J. Chung, "Compact antenna with U-shaped open-end slot structure for multi-band handset applications," *IEEE Transactions on Antennas and Propagation*, Vol. 62, No. 2, 929–932, 2014.
11. Lu, J.-H. and J.-L. Guo, "Small-size octaband monopole antenna in an LTE/WWAN mobile phone," *IEEE Antennas and Wireless Propagation Letters*, Vol. 13, 548–551, 2014.
12. Chang, T.-N. and S.-Y. Cheng, "Ultra wide miniaturized printed antenna," *Electromagnetics*, Vol. 37, 345–354, June 2017.
13. Tsai, P.-C., D.-B. Lin, H.-P. Lin, I.-T. Tang, and P.-S. Chen, "Printed inverted-F monopole antenna for internal multi-band mobile phone antenna," *73rd IEEE Vehicular Technology Conference (VTC Spring)*, Budapest, Hungary, May 2011.